

Preparation and characterization of cobalt oxides nanoparticles starting from Co(II) carboxylate precursors

O. STEFANESCU*, C. DAVIDESCU, C. MUNTEAN

Politehnica University Timisoara, Applied Chemistry and Inorganic Compounds Engineering, 6 Vasile Parvan Blvd., 300223, Timisoara, Romania,

We have successfully used new Co(II) carboxylate compounds for the preparation of nanocrystalline cobalt oxide powders. The Co(II) carboxylate compounds were obtained in the redox reaction between $\text{Co}(\text{NO}_3)_2 \cdot 6\text{H}_2\text{O}$ and diol (1,2-ethandiol and 1,3-propanediol). Co(II) carboxylate compounds with different structures can be obtained depending on the starting material (diol) and the synthesis parameters. As a result, different crystalline phases can be obtained by appropriate thermal treatment: Co_3O_4 , CoO and metallic Co. The redox reaction between the NO_3^- ion and diol takes place at 90°C . Depending on the $\text{Co}(\text{NO}_3)_2 \cdot 6\text{H}_2\text{O}$ – diol system and the molar ratio of the reagents, the redox reaction can be controlled, with isolation of the Co(II) complex combination as pink powder or a burning process can take place, leading to a grey powder. Thermal decomposition of the isolated Co(II) complex combination, at 350°C , leads to CoO, Co_3O_4 or cobalt oxides mixtures. The Co(II) complex combination was characterized by thermal analysis and FT-IR spectrometry. The phase evolution and morphology of the oxides powders were studied by X-ray diffraction and Scanning Electron Microscopy.

(Received April 9, 2015; accepted June 24, 2015)

Keywords: Carboxylate precursor, Cobalt oxides, Redox reaction, XRD

1. Introduction

Transition metal oxides are a well-studied class of materials due to their particular properties and applications in various fields, such as heterogenous catalysis [1], gas sensing [2], electrochemical devices and solar energy transformation [3-5]. One such system comprises cobalt oxides of different composition and stoichiometry, relying on the close thermodynamic stability of the $\text{Co}^{2+}/\text{Co}^{3+}$ oxidation states. Cobalt oxides show catalytic activity in surface reactions and partial oxidation, which depend on the redox properties of the metal. The close thermodynamic stability of Co^{2+} and Co^{3+} is the key feature in these mechanisms [6]. Among all known types of cobalt oxides known until now, Co_3O_4 and CoO are the most stable and useful in the industry [7, 8]. Even though CoO is stable at high temperatures, bulk particles may easily exist at environmental temperature and oxygen partial pressure. CoO is an antiferromagnetic material which is well studied due to its magnetic characteristics [9, 10] and applications as gas sensor [11, 12]. One of the most important applications of CoO is in the field of Ni/H₂ and Ni/Cd batteries, in which it plays the role of enhancing the discharge deepness and enlarging the current [13]. In the past few years CoO became more attractive due to results as photocatalyst used for water decomposition under influence of solar light [5]. Due to the bandgap of 2.4 eV, CoO presents a high photocatalytic activity. In order to take full advantages of CoO in this field, the material has to present unique features such as high purity,

high density, high stability, ultrafine diameter, monodispersion and nano-scale size [14].

On the other hand, the spinel type Co_3O_4 is an important technological material with applications as solar selective absorber, hydrocracking catalyst, in pigment glasses, photocatalysis and ceramics [15-20]. When falling in the nanosized regime, Co_3O_4 is expected to lead to even more attractive applications. In the past few years, interest has been devoted to the synthesis of Co_3O_4 nanostructures with different morphologies: nanoparticles, nanowires, nanotubes [21-24]. In the last years Co_3O_4 has been prepared by different techniques such as combustion method, hydrothermal method, sol-gel process, spray pyrolysis, coprecipitation [25-29]. One of the most used soft chemical methods for preparation of nanoscale Co_3O_4 is the thermal decomposition method due to the process simplicity, short reaction time, low temperature and easy work-up [22, 30, 31]. The most important issue of this topic is to design a precursor which would allow the synthesis of the desired nanomaterials at a low temperature and with directed properties [22].

In our previous papers we reported an original route for the synthesis of carboxylate compounds, which are precursors of simple and mixed oxides in nanometer range [32-34]. The synthesis method consists in a redox reaction of diols with some metallic nitrates leading to different metal carboxylates, depending on the diols nature and the molar ratio NO_3^- : diol. Such compounds decompose at relatively low temperatures, forming the simple or mixed oxides with evolving of volatile products (CO, CO₂, H₂O).

The method is versatile making it possible to obtain different precursors by varying the experimental conditions.

Because CoO and Co₃O₄ represent oxides which are difficult to obtain as single phases, our paper reports the synthesis of these oxides by ranging the experimental procedure based on the thermal decomposition of Co(II) carboxylates, obtained during the redox reaction of 1,2-ethandiol and 1,3-propanediol, respectively, with cobalt nitrate.

2. Experimental

The starting materials were Co(NO₃)₂·6H₂O, 1,2-ethandiol (OH(CH₂)₂OH), 1,3-propanediol (OH(CH₂)₂CHOHCH₃) and nitric acid (65 wt%) with analytical grade, provided from Merck Co. The Co(II) carboxylate compound (precursor) was prepared by dissolving Co(NO₃)₂·6H₂O in 1,2-ethandiol (EG) and 1,3-propanediol (1,3PG), respectively, to which 3 drops of nitric acid were added, under magnetic stirring (Fig.1a). The Co(NO₃)₂·6H₂O amounts were calculated for 2 g CoO and are given in Table 1. The molar ratio NO₃⁻: diol was calculated taking into account the reaction stoichiometry for the formation of the following carboxylates: oxalate (sample E1), glyoxylate (sample E2), malonate (samples P1 and P2) – Eq. 1-3.

Table 1. Syntheses characteristics

Sample	Diol	Quantity/mole			Molar ratio NO ₃ ⁻ : Diol	Type of complex combination
		Co(NO ₃) ₂ ·6H ₂ O	NO ₃ ⁻	Diol		
E1	EG	0.0267	0.0534	0.0200	1:0.375	oxalate
E2		0.0267	0.0534	0.0267	1:0.5	glyoxylate
P1	1,3PG	0.0267	0.0534	0.0200	1:0.375	malonate
P2		0.0267	0.0534	0.0250 (25% excess)	1:0.469	malonate

By heating the sample solutions, the redox reaction between the NO₃⁻ anions and the -OH groups of the diol, was initiated at 90°C with evolving of brown nitrogen oxides (NO_x). The synthesis procedure was conducted under controlled heating, with isolation of a Co(II) complex combination, as pink powder, starting from sample E1 (Fig.1b). The obtained powder was heated at 130°C, 2h, until the redox reaction was finished and has been analyzed by FTIR spectrometry and thermal analysis. The dried powder was annealed at 350°C and 1000°C, 3h in ambient air.



Fig.1: a.) Co(NO₃)₂·6H₂O – diol solution;
b.) Powder – isolated complex combination;
c.) Powder – burning of the complex combination

For the samples E2, P1 and P2, the redox reaction with formation of Co(II) complex combination took place simultaneous with the organic ligands burning leading to a magnetic grey black powder (Fig.1c).

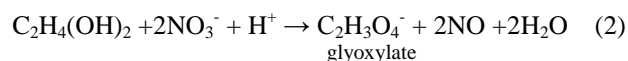
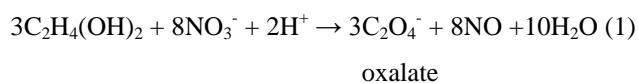
Thermal analysis, for description of the redox reaction evolution, was performed on a 1500D MOM Budapest derivatograph by deposition of a reactants solution thin layer on plate like Pt crucibles. The experiment was carried out, in air, under identical conditions with the instrumental parameters: heating rate 5°C/min up to 500°C, sample mass 100 mg and reference material for DTA was α-Al₂O₃. Infrared spectra of the powders were recorded on Shimadzu Prestige-21 FT-IR system in the range of 400–4000 cm⁻¹ using KBr pellets.

Thermal analysis for examination of the synthesized powders was performed on a 1500D MOM Budapest derivatograph in air with the heating rate of 5 °C/min up to 500 °C. The phase evolution was investigated by Rigaku Ultima IV X-ray diffractometer using monochromatic CuKα radiation (λ = 1.54056 Å). The average crystallite size was calculated using the whole pattern profile fitting method (WPPF). The instrument influence has been subtracted using the diffraction pattern of a Si standard recorded in the same conditions. The crystalline phases were identified using JCPDS-ICDD files.

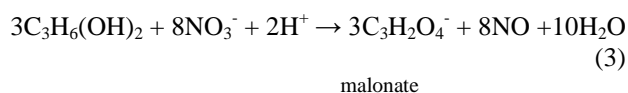
The morphology and microstructure of the particles were observed by scanning electron microscopy (SEM) using a FEI QUANTA FEG 250 microscope (operating at 30 kV and 7 mm working distance).

3. Results and discussion

The redox reaction between 1,2-ethandiol and cobalt nitrate occurs with oxidation of OH(CH₂)₂OH by the NO₃⁻ ions to carboxylate anions (oxalate, glyoxylate) depending on the molar ratios [35] according to the equations below:



The redox reaction between 1,3-propanediol and cobalt nitrate occurs with oxidation of OH(CH₂)₂CHOHCH₃ by the NO₃⁻ ions only to the malonate anion [33].



The mechanism of the redox reaction, for the formation of the complex combinations, was studied by thermal analysis. Figure 2 and 3 present TG and DTA curves for the cobalt nitrate – EG (sample E1) and cobalt nitrate – 1,3PG (sample P1) solutions.

The evolution of the DTA curves is similar in both cases and shows exothermic effects at 105 °C and 120 °C corresponding to the redox reaction NO_3^- - diol with formation of oxalate and malonate type Co(II) complex combinations [36].

The exothermic effects from 240 °C and 250 °C can be assigned to the oxidative decomposition of the formed complex combinations. Taking into account the results of thermal analysis, 140 °C was chosen as synthesis temperature for the Co(II) oxalate type complex combination.

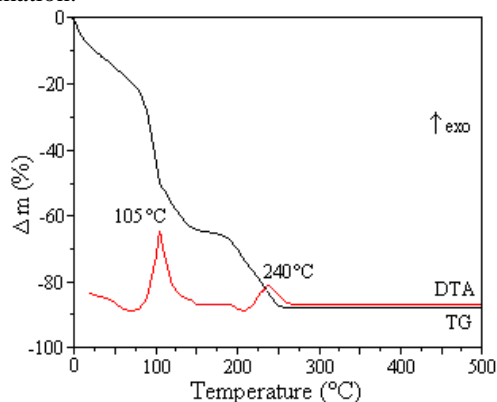


Fig. 2. TG and DTA curves for the solution $\text{Co}(\text{NO}_3)_2 \cdot 6\text{H}_2\text{O} - \text{EG}$ (sample E1)

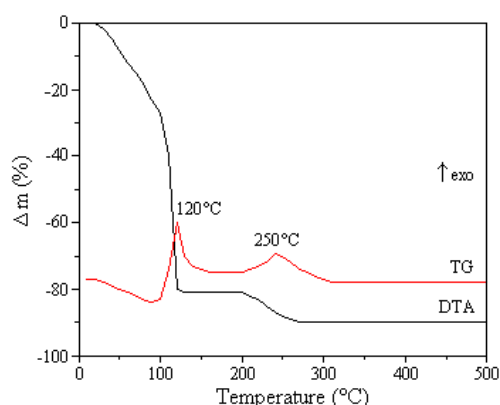


Fig. 3. TG and DTA curves for the solution $\text{Co}(\text{NO}_3)_2 \cdot 6\text{H}_2\text{O} - 1,3\text{PG}$ (sample P1)

The IR spectrum of the compound E1 synthesized at 140 °C (Fig.4) shows an intense and large band in the range 3000 – 3600 cm^{-1} with a maximum at 3369 cm^{-1} , due to the vibration $\nu(\text{OH})$ from coordinated water as well as due to strong hydrogen bonds of the water molecules with the oxalate ligand. The absorption bands from 828 cm^{-1} and 714 cm^{-1} confirm also the presence of water in coordinated form [37]. The intense band at 1636 cm^{-1} is attributed to the vibration $\nu_{\text{asym}}(\text{OCO})$ and the value shows that the Co(II)-carboxylate bond is preponderant ionic [38, 39]. The band at 1387 cm^{-1} is assigned to the vibration $\nu_{\text{sym}}(\text{OCO})$ [40]. The difference between the values of ν_{asym} and ν_{sym} being 249 cm^{-1} (higher than 170 cm^{-1}), shows that the metal-carboxylate bond is preponderantly ionic, and the carboxylate group acts like bidentate ligand [41]. At

the same time, the value for $\nu_{\text{sym}}(\text{OCO})$ at 1387 cm^{-1} and $\delta(\text{OCO})$ at 1314 cm^{-1} , are in agreement with the position of the corresponding absorption in the oxalate bridged Co(II) complex [42]. The sharp band from 492 cm^{-1} is attributed to the vibration $\nu(\text{Co-O})$ and $\nu(\text{C-C})$ [43].

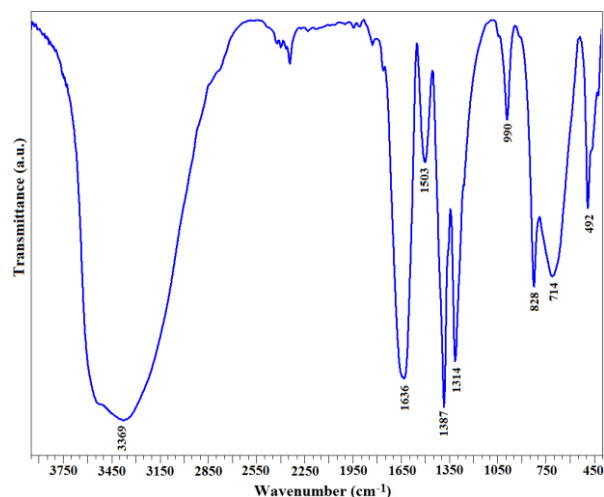


Fig. 4. FTIR spectrum of sample E1 synthesized at 140 °C

Fig 5 presents the thermal behaviour of the oxalate type compound E1 synthesized at 140 °C. From the evolution of the TG and DTA thermal curves one can see two different steps of mass loss on TG. In the temperature range 175 - 200 °C the mass loss, with an endothermic effect, indicates the elimination of the coordinated water molecules. In the temperature range 200 – 270 °C the mass loss is attributed to the exothermic decomposition of anhydrous oxalate. Up to 500 °C the mass remains constant and the residue are cobalt oxides (Co_3O_4 and/or CoO).

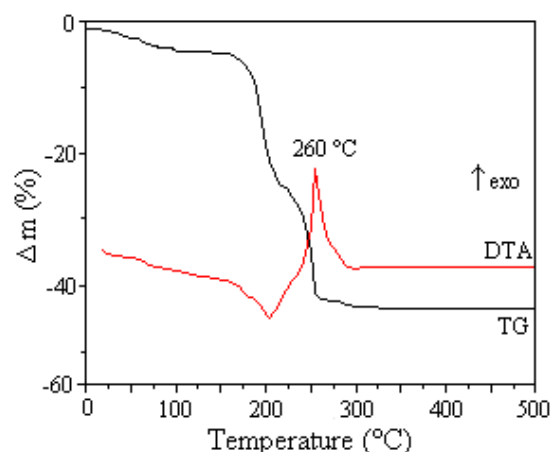


Fig. 5. TG and DTA curves for sample E1 synthesized at 140 °C

The samples E2 (glyoxylate type), P1 and P2 (malonate type) could not be isolated because of the lower thermal stability of the glyoxylate and malonate ligands from the complex combinations and the autocatalytic

effect of the Co ion. The redox reactions started at 90°C with NO_x evolving when the complex combinations were formed, in situ, followed by immediate burning with generation of a reducing environment (CO, C). In case of E2 the burning of the complex combination took place with incandescence while for P1 and P2 the burning was with flame (combustion). The behaviour of the samples P1 and P2, synthesized with 1,3PG, is due to the longer organic chain as well as to the higher reducing character of this diol compared to EG.

Figure 6 presents the XRD patterns of the products resulted from the burning of the glyoxylate type sample E2 at 90°C and by annealing of the oxalate type sample E1 at 350 and 1000°C. The pattern of sample E2 shows the well-crystallized, single phase, CoO. The molar ratio NO_3^- : EG for the formation of the glyoxylate type complex, by the reducing environment created during the burning initiated at 90°C, is optimal for the obtaining of the single phase CoO. The average size of the CoO crystallites resulted from XRD data is 30 nm. The pattern of the sample E1 annealed at 350°C indicates as well-crystallized, single phase, Co_3O_4 with nanoparticles having an average diameter of 14 nm. The formation of this phase is due to the isolation of the oxalate type complex combination followed by thermal decomposition at a predefined temperature (350°C). By annealing of the sample E1 at a higher temperature (1000°C) Co_3O_4 is stabilized. With temperature increase there is an increase of the mean particle size to ~ 70 nm.

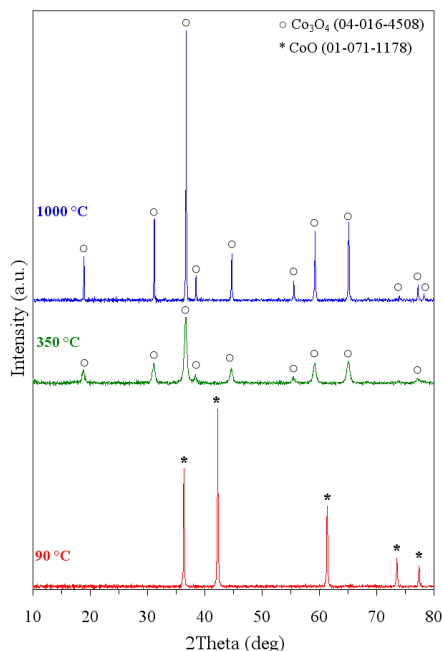


Fig. 6. XRD patterns of the products obtained from different heating of samples E1 and E2

The XRD pattern (Fig. 7) of the product resulted, from the burning at 90°C, of the malonate type sample P1 shows a mixture of phases where CoO is predominant. The

formation of this phase is due to the precursor type, the reducing environment and the burning temperature. By annealing of sample P1 at 350°C CoO transforms to Co_3O_4 while in the sample annealed at 1000°C, Co_3O_4 is the single phase. The particles size is nanometric, ranging from 20 to 100 nm depending on the temperature of the thermal treatment.

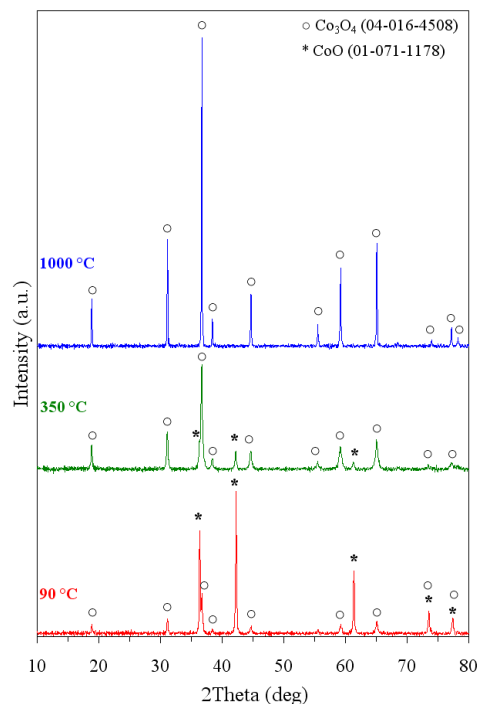


Fig. 7. XRD patterns of the products obtained from different thermal treatments of sample P1

Fig. 8 presents the XRD pattern of sample P2, synthesized with an excess of 1,3PG, showing a mixture of metallic Co and CoO. This is due to the nature of the precursor (malonate), the molar ratio NO_3^- : 1,3PG and the reducing atmosphere created during the short time burning of the complex combination.

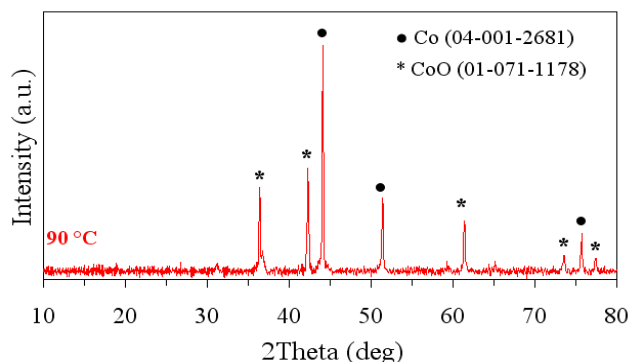


Fig. 8. XRD patterns of the product obtained from burning of sample P2

From thermal analysis data (Fig. 9) one can determine the content of metallic Co in the phase mixture. The TG curve shows no mass variation up to 400°C. In the temperature range 450 – 700°C, the TG curve shows a mass increase corresponding to the oxidation of Co and CoO to Co₃O₄.

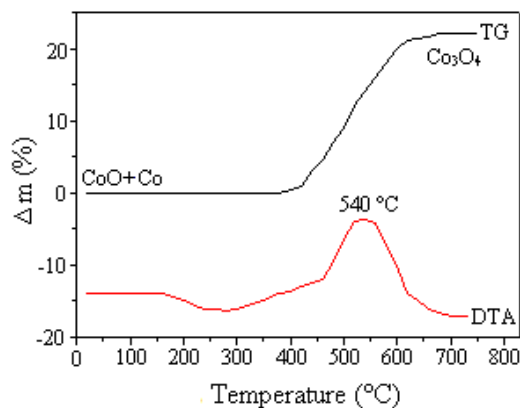


Fig. 9. TG and DTA curves of the product obtained from burning of sample P2

Inspection of the SEM figures, for sample E1 annealed at 350 °C (Fig. 10 a) and 1000 °C (Fig. 10 b), manifests that the prepared spinel Co₃O₄ shows a porous network as a consequence of the gases escaping during synthesis. It is obvious that the nanoparticles are uniform hollow tubular shapes with voids and holes randomly distributed among them. The particles are agglomerated with sizes ranging from 20 nm for the sample annealed at 350 °C to 70 μm for the sample annealed at 1000 °C.

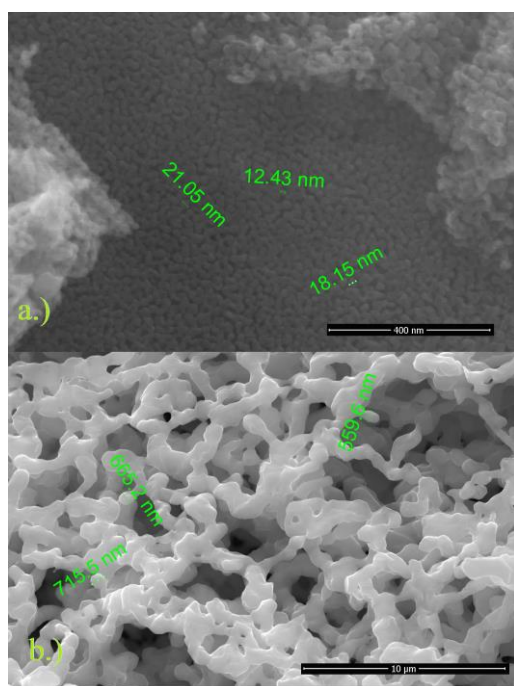


Fig. 10. SEM images of sample E1 annealed at 350 °C (a) and 1000 °C (b)

The SEM image of the product resulted (CoO) from the burning of sample E2 (Fig. 11) reveals a sintering tendency of irregular particles due to a fast temperature increase during synthesis. The average particle size is in the nanometer range.

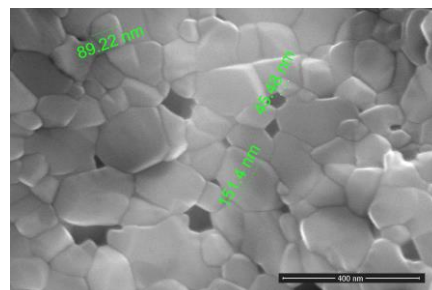


Fig.11. SEM image of the product resulted from burning of sample E2

4. Conclusions

The study presented a new procedure for the obtaining, at low temperatures, of CoO and Co₃O₄ nanoparticles as single phases, starting from Co(II) carboxylate compounds precursors. The diol content and its structure (reducing agent) are key factors that control the formation of reduced oxidation states compounds, such as CoO. The ratio of the diol to nitrate dramatically influenced the phase formation of the final products and the particle size. The synthesized cobalt oxides nanoparticles are meant to be used for photocatalytic applications, which are strongly influenced on the particle size and the lattice structure.

Acknowledgements

This work was partially supported by the strategic grant POSDRU/159/1.5/S/13707 (2014) of the Ministry of National Education, Romania, co-financed by the European Social Fund – Investing in People, within the Sectoral Operational Programme Human Resources Development 2007-2013.

References

- [1] A. Zecchina, D. Scarano, S. Bordiga, G. Spoto, C. Lamberti, *Adv. Catal.* **46**, 265 (2001).
- [2] N. Barsan, D. Koziej, U. Weimar, *Sens. Actuators.* **B121**, 18 (2007).
- [3] S.L. Chou, J.Z. Wang, H.K. Liu, S.X. Dou, *J. Power Sources* **182**, 359 (2008).
- [4] H. Cao, S.L. Suib, *J. Am. Chem. Soc.* **116**, 5335 (1994).
- [5] L. Liao, Q. Zhang, Z. Su, Z. Zhao, Y. Wang, Y. Li, X. Lu, D. Wei, G. Feng, Q. Yu, X. Cai, J. Zhao, Z. Ren, H. Fang, F. Robles-Hernandez, S. Baldelli, J. Bao, *Nature Nanotech.* **9**, 69 (2014).

- [6] S.C. Petitto, E.M. Marsh, G.A. Carson, M.A. Langell, *J. Molec. Catal. A* **281**, 49 (2008).
- [7] M. Verelst, T. Ould Ely, C. Amiens, E. Snoeck, P. Lecante, A. Mosset, M. Respaud, J.M. Broto, B. Chaudret, *Chem. Mater.* **11**, 2702 (1999).
- [8] D. Wegner, Z. Inglot, K.P. Lieb, *Hyperf. Interact.* **59**, 313 (1990).
- [9] A. Berger, M.J. Pechan, R. Compton, J.S. Jiang, J.E. Perason, S.D. Bader, *Phys. Rev. B* **306**, 235 (2001).
- [10] M. Rubinstein, P. Lubitz, S.F. Cheng, *J. Magn. Magn. Mater.* **195**, 299 (1999).
- [11] N. Koshizaki, K. Yasumoto, T. Sasaki, *Nanostruct. Mater.* **12**, 971 (1999).
- [12] C.W. Tang, C.B. Wang, S.H. Chien, *Thermochim. Acta* **473**, 68 (2008).
- [13] M. Oshitani, H. Yufu, K. Takashima, S. Tsuji, Y. Matsumaru, *J. Electrochem. Soc.* **136**, 1590 (1989).
- [14] W. Wang, G. Zhang, *J. Cryst. Growth* **311**, 4275 (2009).
- [15] C.N.P. Fonseca, M.A. Depaoli, A. Gorenstein, *Sol. Energy Mater. Sol. Cells* **33**, 73 (1994).
- [16] K. Venkateswara Rao, C.S. Sunandana, *Solid State Comm.* **148**, 32 (2008).
- [17] J. Jansson, A.E.C. Palmqvist, E. Fridell, *J. Catal.* **211**, 387 (2002).
- [18] S.D. Choi, B.K. Min, *Sens. Actuators B* **77**, 330 (2001).
- [19] W.Y. Li, L.N. Xu, J. Chen, *J. Adv. Funct. Mater.* **15**, 851 (2005).
- [20] X. Lou, J. Han, W. Chu, X. Wang, Q. Cheng, *Mater. Sci. Eng. B* **137**, 268 (2007).
- [21] L. Sun, H. Li, L. Ren, *Solid State Sci.* **11**, 108 (2009).
- [22] S. Farhadi, J. Safabakhsh, P. Zaringhadam, *J. Nanostruct. Chem.* **3**, 69 (2013).
- [23] J. Du, L. Chai, G. Wang, K. Li, Y. Quian, *Aust. J. Chem.* **61**, 153 (2008).
- [24] R. M. Wang, C.M. Liu, H.Z. Zhang, C.P. Chen, L. Guo, H.B. Xu, S.H. Yang, *Appl. Phys. Lett.* **85**, 2080 (2004).
- [25] F. Gu, C. Li, Y. Hu, L. Zhang, *J. Cryst. Growth* **304**, 369 (2007).
- [26] E. Lester, G. Aksomaityte, J. Li, S. Gomez, J. Gonzalez-Gonzalez, M. Poliakoff, *Prog. Cryst. Growth Charact. Mater.* **58**, 3 (2012).
- [27] M.E. Baydi, G. Poillerat, J.L. Rehspringer, J.L. Gautier, J.F. Koenig, P. Chartier, *J. Solid State Chem.* **109**, 281 (1994).
- [28] D.Y. Kim, S.H. Ju, H.Y. Koo, S.K. Hong, Y.C. Kangf, *J. Alloys Compd.* **417**, 254 (2006).
- [29] J. Pal, P. Chauhan, *Mat. Char.* **61**, 575 (2010).
- [30] L. Ren, P. Wang, Y. Han, C. Hu, B. Wei, *Mater. Phys. Lett.* **476**, 78 (2009).
- [31] K. Thangavelu, K. Prameswari, K. Kuppusamy, Y. Haldorai, *Mater. Lett.* **65**, 1482 (2011).
- [32] O. Stefanescu, T. Vlase, G. Vlase, N. Doca, M. Stefanescu, *Thermochim. Acta* **519**, 22 (2011).
- [33] O. Stefanescu, M. Stefanescu, *J. Organomet. Chem.* **740**, 50 (2013).
- [34] M. Stefanescu, C. Caizer, M. Stoia, O. Stefanescu, *J. Optoelectron. Adv. Mater.* **7**, 607 (2005).
- [35] M. Birzescu, Complexes combinations with ethyleneglycol and their oxidation products, PhD Thesis, Bucharest University, (1998)
- [36] M. Birzescu, M. Niculescu, R. Dumitru, O. Carp, E. Segal, *J. Therm. Anal. Calorim.* **96**, 979 (2009).
- [37] M. Brezeanu, L. Patron, O. Carp, M. Andruh, N. Stanica, *Rev. Roum. Chim.* **36**, 545 (1991).
- [38] K. Nakamoto, Y. Morimoto, A.E. Martell, *J. Am. Chem. Soc.* **83**, 4528 (1961).
- [39] B.S. Randhawa, K. Gandotra, *J. Therm. Anal. Calorim.* **85**, 417 (2006).
- [40] B.S. Randhawa, M. Kaur, *J. Therm. Anal. Calorim.* **89**, 251 (2007).
- [41] M. Niculescu, N. Vaszilcsin, M. Birzescu, P. Budrugaec, E. Segal, *J. Them. Anal. Calorim.* **65**, 881 (2001).
- [42] I. Luisetto, F. Pepe, E. Bemporad, *J. Nanopart. Res.* **10**, 59 (2008).
- [43] C.F. Windisch, G.J. Exarhos, R.R. Owings, *J. Appl. Phys.* **95**, 5435 (2004).

* Corresponding author: oanaelenastefanescu@yahoo.com